Modeling of Multicomponent Drying of Polymer Films

Sacide Alsoy and J. Larry Duda
Center for the Study of Polymer-Solvent Systems, Dept. of Chemical Engineering,
The Pennsylvania State University, University Park, PA 16802

The drying of volatile solvents from a coated film is a complicated process since it involves simultaneous heat and mass transfer controlled by complex transport and thermodynamic behavior of polymer solutions. In this work, a model is developed to describe the drying behavior of multicomponent polymer solutions deposited on the impermeable substrate. A key component of the model is incorporation of multicomponent diffusion coefficients that consist of thermodynamic factors and self-diffusivities. Vrentas-Duda free-volume theory was used for predicting concentration and temperature dependency of self-diffusion coefficients. Drying processes in ovens with different zones in which temperature, velocity, and/or partial pressure of each solvent vary from zone to zone are considered. The predictions from the models provide detailed information about the relative importance of internal and external resistances to drying, effect of operating conditions, effect of the multiple-zone approach, as well as sensitivity of all physical properties on the drying rate. The validity of the model was confirmed by comparing predictions with the drying data available in the literature and the data collected in our laboratories. The experimental data and the simulation results are in good agreement.

Introduction

Drying of solvent-coated polymer films is a key unit operation in the economic production of many polymeric products, including photographic films, synthetic fibers, adhesives, magnetic media, and book coverings. The coatings are produced by casting a continuous single layer of polymer solution or multiple distinct solution layers onto a moving substrate and to form the final product these layers are dried in an oven with forced-air convection. The structure and properties of the final product are greatly influenced by the course of drying. Today, coating technology is facing many problems in the production of coated webs such as phase separations, unwanted internal gradients, inappropriate nonuniformities and various kinds of defects that can be attributed to the poorly chosen drying conditions. Therefore, the accurate modeling of this process becomes crucial for process design and optimization.

The removal of volatile solvents from a coated film is a complex process of heat and mass transfer within the shrinking film as well as simultaneous mass and heat transfer from the interfaces. Vapor–liquid equilibria at the polymer-film–gas interface, diffusion coefficients that strongly depend on temperature and concentration, and the state of the polymer all complicate the process. Many models for drying the binary polymeric solutions exist in the literature (Hansen, 1968; Okazaki et al., 1974; Blandin et al., 1987a,b; Yapel, 1988; Waggoner and Blum, 1989; Vrentas and Vrentas, 1994; Cairncross et al., 1995; Gutoff, 1996). However, models for multicomponent drying of polymer films are very limited. The main reasons for this are the difficulty in handling complex transport equations and the lack of information about the diffusion coefficients in multicomponent systems.

In an earlier study, Yapel (1988) developed a model for a coating containing any number of components on a base stock. In his model, mass-transfer process was analyzed using mass average velocity, and temperature profile within the coating and substrate were predicted by solving the unsteady-state heat-transfer equations. An isothermal one-dimensional convection diffusion reaction equation was developed by Cairn-

Correspondence concerning this article should be addressed to J. L. Duda.

cross et al. (1996) for predicting drying in coatings that react and gel. In both of these studies, diffusive flux is described by Fick's law for multicomponent solutions with the cross-term diffusion coefficients set to zero, and the main diffusion coefficients are approximated by corresponding self-diffusion coefficients. In Yapel's work, the temperature and concentration dependency of self-diffusion coefficients are predicted from Vrentas–Duda (Vrentas and Duda, 1977a,b; Duda et al., 1982; Vrentas et al., 1985a) free-volume theory, while in Cairncross the work diffusion coefficient of each species is assumed to be constant and equal. A more complete model has been developed for the formation of asymmetric membranes that incorporates both main and cross-diffusion coefficients in describing the diffusive flux (Shojaeia et al., 1994). The model predicts the evaporation of both solvent and nonsolvent from an initially homogeneous polymer/solvent/nonsolvent system. It was applied to a well-characterized cellulose acetate/acetone/water system for which sufficient experimental data were available to permit the determination of both main and cross-diffusion coefficients. Additional complexity was introduced into the model equations, since the mass-transfer process was analyzed using the mass average velocity, which causes a need for including the convective term.

In the first part of this work, a multicomponent drying model is developed to predict drying behavior of polymer solutions on inert substrates. This analysis utilizes several concepts that were incorporated in the analysis of a binary polymer solution as presented by Alsoy and Duda (1998), and the precursor article of Vrentas and Vrentas (1994). Specifically, the problem is cast in terms of the volume-average velocity instead of the mass-average velocity. This significantly reduces the complexity of the governing equations when the polymer and solvents have different densities and when the coating is nonreactive. Also, the temperature gradient in the polymer and substrate layers are neglected based on the detailed analysis of Yapel (1988), in which it is shown that under typical commercial drying conditions, the resistance to heat transfer is much greater in the gas phase than in either the polymer or substrate layers. The numerical analysis of the governing equations is based on the finite difference technique previously utilized by Alsoy and Duda (1998). This incorporates an immobilization of the moving boundary and a variable grid spacing to minimize the number of equations required to describe the very steep concentration gradients that typically form near the gas–polymer-solution interface. As a consequence, the procedures utilized in this study greatly reduce the computer power required to accurately describe the complex drying process, and the results presented in this study were obtained utilizing a UNIX-based workstation instead of the supercomputer facilities required by some previous investigators.

In the formulation of the problem, the most critical step involves the description of a multicomponent diffusion process. The multicomponent diffusion theory derived by Alsoy (1998) is used to relate self-diffusion coefficients to mutual diffusion coefficients in the ternary system. The most important parameters in the model are the multidiffusion coefficients that for most polymer systems are strong functions of temperature and concentration. The free-volume theory of Vrentas and Duda (1977a,b) was utilized to describe the influence of temperature and concentration on the self-diffusion coefficients, and a ternary Flory–Huggins model (Flory, 1953; Favre et al., 1996) was utilized to describe the thermodynamics of the multicomponent system. In this thermodynamic model, the vapor pressures of the pure solvents were predicted by the Antoine equation correlation of Daubert and Danner (1994). It should be noted that not only is the thermodynamics of the ternary system of importance for describing the vapor pressure of the solvent at the polymer-solution–vapor interface, but the ternary system thermodynamics is also required for determining the concentration and temperature dependencies of the mutual diffusion coefficients.

In the second section of this work, the model is applied to polystyrene/toluene/tetrahydrofurane, polystyrene/toluene/benzene and polystyrene/toluene/ethylbenzene systems. Simulations have been conducted for different cases to illustrate the power of the model and wealth of information that cannot be obtained otherwise. The model predictions are compared with the experimental data collected for the systems mentioned earlier.

It should be emphasized here that the model developed in this work does not take into account all the complexities involved during the drying process. Specifically, the model can only be applied to nonreactive coatings, and any possible complication associated with the coupling of the diffusion process with the relaxation of polymer chains is neglected. Furthermore, phase separation is not considered.

Theory

The drying geometry is given in Figure 1. Initially the polymer film has a constant thickness L and extends from $x = 0$ to $x = X(t)$. The substrate has a constant thickness H. The gas phase next to the polymer layer has a temperature T^G and heat-transfer coefficient h^G, and the gas phase next to the substrate has a temperature T^g and heat transfer coefficient h^g. The polymer film consists of a polymer dissolved in more than one solvent.

Using this geometry and notation given in Figure 1, model equations are derived as follows.

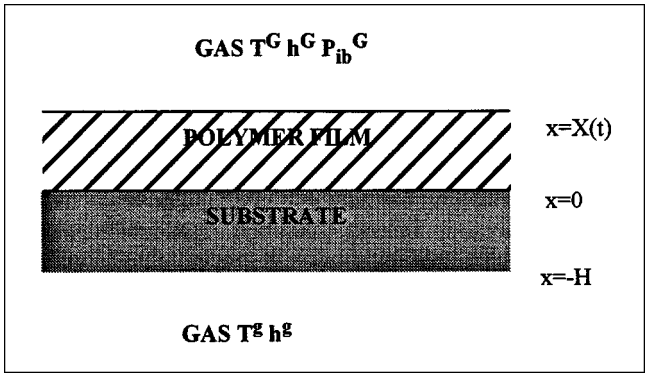

Figure 1. The drying geometry.

Species continuity equation for component i:

$$\frac{\partial \rho_i^p}{\partial t} = \frac{\partial}{\partial x}\left(\sum_{j=1}^{N-1} D_{ij}^p \frac{\partial \rho_j^p}{\partial x} \right) - \frac{\partial \left(\rho_i^p v^{\neq} \right)}{\partial x} + R_i, \qquad (1)$$

in which the mass transfer is assumed to be one-dimensional and the generalized Fick's law is used in describing the flux equations for the multicomponent system. If Eq. 1 is multiplied by the partial specific volume of the corresponding component and the resulting equation is summed over all species, and if it is assumed that there is no volume change on mixing, then the following expression is obtained for the gradient of volume-average velocity.

$$\frac{\partial v^{\neq}}{\partial x} = \sum_{j=1}^{N} R_j \hat{V}_j^p. \qquad (2)$$

In previous work, the gradient of volume-average velocity is set to zero, since it is assumed that all the reactions are volume conserving, which results in zero volume-average velocity everywhere in the coating (Cairncross et al., 1996). However, in this work, the gradient of volume-average velocity becomes zero only for nonreactive coatings.

Heat-transfer equation in polymer solution and substrate

$$\frac{dT}{dt} = -\left[\frac{h^G \left(T - T^G \right) + \sum_{i=1}^{N-1} k_i^G \Delta \hat{H}_{vi} \left(P_{ii}^G - P_{ib}^G \right) + h^g \left(T - T^g \right)}{\rho^p \hat{C}_p^p X(t) + \rho^s \hat{C}_p^s H} \right], \qquad (3)$$

in which a single uniform temperature for the polymer film and the substrate layer are assumed, since the gas-phase convective resistance to heat transfer is much greater than the conductive resistance in the polymer and substrate layers. Also, average values for densities, heat capacities, and thermal conductivities of polymer solution and substrate are used and radiative heat-transfer mode is neglected.

Time dependence of boundary position

$$\frac{dX}{dt} = v^{\neq} - \left[\frac{\sum_{i=1}^{N-1} J_i^{p \neq} \hat{V}_i^p}{\left(1 - \sum_{i=1}^{N-1} \rho_i^p \hat{V}_i^p \right)} \right]. \qquad (4)$$

This equation is derived from a jump mass balance for the polymer (Alsoy, 1998). The equations just derived were solved for the nonreactive-coating case, since there is no experimental data available on reactive coatings and associated reaction kinetics. For this case from Eq. 2, the gradient of volume-average velocity becomes zero, resulting in zero volume-average velocity everywhere in the polymer film, since it is zero at the substrate–polymer interface. The boundary and initial conditions can be derived as follows:

Boundary Conditions:

$$x = 0: \qquad \frac{\partial \rho_i^p}{\partial x} = 0 \qquad (5)$$

$$x = X(t) \qquad -\left[\sum_{j=1}^{N-1} D_{ij}^p \frac{\partial \rho_j^p}{\partial x} \right] - \rho_i^p \frac{dX}{dt} = k_i^G \left(P_{ii}^G - P_{ib}^G \right). \qquad (6)$$

Initial Conditions:

$$\rho_i^p(0, x) = \rho_{io}^p \qquad (7)$$

$$X(0) = L \qquad T(0) = T_o. \qquad (8)$$

To facilitate numerical treatment of the moving interface, the following coordinate transformation is used:

$$\eta = \frac{x}{X(t)}. \qquad (9)$$

In addition, the system of equations can be nondimensionalized using the following dimensionless variables:

$$T^* = \frac{T - T_o}{T^G - T_o} \qquad (10)$$

$$C_i = \frac{\rho_i^p}{\rho_{io}^p} \qquad (11)$$

$$t^* = \frac{t D_{11,o}^p}{L^2} \qquad (12)$$

$$X^* = \frac{X(t)}{L}. \qquad (13)$$

Inserting Eqs. 10, 12, and 13 in Eq. 3 results in the following dimensionless form of the heat-transfer equation for the coating and substrate:

$$\frac{dT^*}{dt^*} = \frac{A(1 - T^*) + E + B}{F + X^*}, \qquad (14)$$

where the constants A, B, E, and F are defined as follows:

$$A = \frac{L\left(h^G + h^g \right)}{D_{11,o}^p \rho^p \hat{C}_p^p} \qquad (15)$$

$$B = -\frac{L \sum_{i=1}^{N-1} k_i^G \Delta \hat{H}_{vi} \left(P_{ii}^G - P_{ib}^G \right)}{\rho^p \hat{C}_p^p D_{11,o}^p \left(T^G - T_o \right)} \qquad (16)$$

$$E = \frac{Lh^g(T^g - T^G)}{D^p_{11,o}\rho^p \hat{C}^p_p (T^G - T_o)} \tag{17}$$

$$F = \frac{\rho^s \hat{C}^s_p H}{\rho^p \hat{C}^p_p L}. \tag{18}$$

Combining Eqs. 1, 9, 11, 12, and 13 yields the following species-continuity equation for component i:

$$\frac{\partial C_i}{\partial t^*} - \frac{\eta}{X^*}\frac{dX^*}{dt^*}\frac{\partial C_i}{\partial \eta} = \frac{1}{X^{2*}}\frac{\partial}{\partial \eta}\left[\sum_{j=1}^{N-1}\frac{D^p_{ij}}{D^p_{11,o}}\frac{\rho^p_{jo}}{\rho^p_{io}}\frac{\partial C_j}{\partial \eta}\right]. \tag{19}$$

The dimensionless form of the time dependence of boundary position and the boundary and initial conditions given by Eqs. 4 through 8 can be rewritten as follows:

$$\eta = 0 \qquad \frac{\partial C_i}{\partial \eta} = 0 \tag{20}$$

$$\eta = 1 \qquad -\frac{1}{X^*}\left[\sum_{j=1}^{N-1}\frac{D^p_{ij}}{D^p_{11,o}}\frac{\rho^p_{jo}}{\rho^p_{io}}\frac{\partial C_j}{\partial \eta}\right] - C_i\frac{dX^*}{dt^*} = \frac{k^G_i(P^G_{ii} - P^G_{ib})L}{\rho^p_{io}D^p_{11,o}} \tag{21}$$

$$\eta = 1 \qquad X^*\frac{dX^*}{dt^*} = \frac{\sum_{i=1}^{N-1}\hat{V}^p_i \sum_{j=1}^{N-1}\frac{D^p_{ij}}{D^p_{11,o}}\frac{\partial C_j}{\partial \eta}\rho^p_{jo}}{\left(1 - \sum_{i=1}^{N-1}\rho^p_{io}C_i\hat{V}^p_i\right)} \tag{22}$$

$$C_i(0,\eta) = 1 \tag{23}$$

$$X^*(0) = 1 \qquad T^*(0) = 0. \tag{24}$$

Although boundary conditions given by Eqs. 21 and 22 are appropriate, to avoid the calculation of concentration derivatives at the surface numerically, it is preferable to use the integrated form of these equations. Integration of Eq. 19 from $\eta = 0$ to $\eta = 1$, and inserting the boundary conditions given by Eqs. 20 and 21, produces the new form of the boundary condition at $\eta = 1$ as follows:

$$\eta = 1 \qquad \frac{d}{dt^*}\left[X^*\int_0^1 C_i d\eta\right] = -\frac{k^G_i(P^G_{ii} - P^G_{ib})L}{\rho^p_{io}D^p_{11,o}}. \tag{25}$$

Also, substitution of the integrated form of Eq. 19 into Eq. 22 and using Eqs. 23 and 24 results in an explicit expression for the dimensionless thickness of the film given by the following equation:

$$X^* = \frac{1 - \sum_{i=1}^{N-1}\rho^p_{io}\hat{V}^p_i}{1 - \sum_{i=1}^{N-1}\rho^p_{io}\hat{V}^p_i\int_0^1 C_i\, d\eta}. \tag{26}$$

Results and Discussion

According to the model discussed here, multicomponent drying characteristics are initially determined by external conditions such as the mass-transfer coefficient of each solvent, heat-transfer coefficients, gas-phase temperature, partial pressure of each solvent in the gas phase, latent heat of vaporization, and the activity of each solvent. Once the external mass-transfer resistance is no longer limiting, the key issue in the prediction is the accurate calculation of diffusion coefficients in the multicomponent solution, especially when these coefficients are a strong function of composition and temperature. Theoretically, diffusion in a ternary system is described by four diffusion coefficients. The prediction of these diffusivities from the most general form of the multicomponent diffusion theory requires knowledge about friction coefficients that provide a link between the self- and mutual-diffusion coefficients in the multicomponent mixtures (Bearman, 1961; Vrentas et al., 1985b). Unfortunately, no experimental measurements are available on these coefficients or how they change as a function of composition. However, when the ratio of friction coefficients are assumed to be constant, diffusivities are only a function of the self-diffusion coefficients and the thermodynamic factor of the corresponding component (Alsoy, 1998). Or, if the friction coefficients are set to zero, then resulting equations are a function of the self-diffusivities and chemical potential gradient of each component in the mixture (Alsoy, 1998). In the simulations, four

Table 1. Alternative Approximations of Ternary Diffusion Coefficients

Case	D_{11}	D_{12}	D_{21}	D_{22}
1	$D_1\left[\frac{\partial \ln a_1}{\partial \ln \rho_1}\right]$	$\frac{\rho_1}{\rho_2}D_1\left[\frac{\partial \ln a_1}{\partial \ln \rho_2}\right]$	$\frac{\rho_2}{\rho_1}D_2\left[\frac{\partial \ln a_2}{\partial \ln \rho_1}\right]$	$D_2\left[\frac{\partial \ln a_2}{\partial \ln \rho_1}\right]$
2	$D_1\left[\frac{\partial \ln a_1}{\partial \ln \rho_1}\right]$	0	0	$D_2\left[\frac{\partial \ln a_2}{\partial \ln \rho_1}\right]$
3	D_1	0	0	D_2
4	$\rho_1(1-\rho_1\hat{V}_1)D_1\left[\frac{\partial \ln a_1}{\partial \rho_1}\right] - \rho_1\rho_2\hat{V}_2 D_2\left[\frac{\partial \ln a_2}{\partial \rho_1}\right]$	$\rho_1(1-\rho_1\hat{V}_1)D_1\left[\frac{\partial \ln a_1}{\partial \rho_2}\right] - \rho_1\rho_2\hat{V}_2 D_2\left[\frac{\partial \ln a_2}{\partial \rho_2}\right]$	$\rho_2(1-\rho_2\hat{V}_2)D_2\left[\frac{\partial \ln a_2}{\partial \rho_1}\right] - \rho_1\rho_2\hat{V}_1 D_1\left[\frac{\partial \ln a_1}{\partial \rho_1}\right]$	$\rho_2(1-\rho_2\hat{V}_2)D_2\left[\frac{\partial \ln a_2}{\partial \rho_2}\right] - \rho_1\rho_2\hat{V}_1 D_1\left[\frac{\partial \ln a_1}{\partial \rho_2}\right]$

Table 2. Free-Volume Parameters Used in Diffusivity Correlations

Parameter		PS* Toluene	PS** Benzene	PS* THF	PS* EB
D_0	cm^2/s	4.82×10^{-4}	4.47×10^{-4}	14.4×10^{-4}	4.61×10^{-4}
E	J/mol	0	0	0	0
K_{11}/γ	$cm^3/g\cdot K$	0.00145	0.00164	0.00075	0.0014
K_{12}/γ	$cm^3/g\cdot K$	0.000582	0.000582	0.000582	0.000582
K_{21}	K	−86.32	−55.66	10.45	−80.01
K_{22}	K	−327	−327	−327	−327
T_{g1}	K	0	0	0	0
T_{g2}	K	0	0	0	0
$\hat{V}_1^*$	cm^3/g	0.917	0.901	0.899	0.946
$\hat{V}_2^*$	cm^3/g	0.85	0.85	0.85	0.85
ξ		0.58	0.51	0.45	0.69
χ		0.354	0.194†	0.34‡	0.363

*Zielinski (1992).
**Hong (1994).
†Ni (1978).
‡Predicted from the semiempirical expression (Bristow and Watson, 1958).

alternative approaches are used in calculating the ternary diffusion coefficients, and equations corresponding to these cases are shown in Table 1. Self-diffusion coefficients were predicted from the Vrentas and Duda free-volume theory (Ferguson and von Meerwall, 1980; Vrentas et al., 1984), and the chemical potential of each component was calculated from the extension of the Flory–Huggings theory for ternary systems (Flory, 1953; Favre et al., 1996). Free-volume parameters used in the predictions are listed in Table 2.

Equations 14 through 18, and Eq. 19 with associated boundary conditions given by Eqs. 20 and 25 are coupled nonlinear differential equations for which analytical solutions cannot be obtained by using standard functions. An implicit finite difference approximation was used to discretize these equations. A variable grid was applied to generate finer mesh near the interface, since the concentration gradients are steeper there (Alsoy, 1998). The model was first applied to a polystyrene (PS)/tetrahydrofurane (THF)/toluene system coated on polyester base. The input data used for the simulation are obtained from Drake and Wang (1989) and are given in Table 3. The results are given in Figures 2 through 7. Figure 2 shows the average concentration of toluene and THF as a function of time. The results indicate that concentration of THF decreases very rapidly and in 40 s all of THF completely disappears. As THF evaporates, the volume of the solution decreases and the concentration of the low-volatility toluene increases to a maximum, and only begins to decrease after 13 s of drying. The residual concentration of toluene trapped in the coating after 100 s of drying is 0.177 g/cm^3. The increase in toluene concentration is due to higher volatility and higher diffusivity of low molecular weight component THF. Since each of the solvents adds free volume to the polymer film, the increase in toluene concentration enhances the removal of THF. Even though the overall mass of toluene decreases initially, its concentration in terms of gram per unit total volume goes through a maximum because of the volume change of the solution due to the loss of THF.

Table 3. Parameters for Polystyrene/Toluene/Tetrahydrofurane Test System

Initial conditions	
Temperature	303 K
Coating thickness	0.00577 cm
Initial composition of solvent 1	0.321 g/cm^3
Initial composition of solvent 2	0.321 g/cm^3
Substrate parameters	
Heat capacity	1.25 $J/g\cdot K$
Density	1.37 g/cm^3
Base thickness	0.003556 cm
Coating parameters	
Heat capacity	2.12 $J/g\cdot K$
Density of polymer	1.083 g/cm^3
Heat of vaporization of the solvent 1	360 J/g
Heat of vaporization of the solvent 2	435 J/g
Operating conditions	
Base-side heat-transfer coefficient	0.9228×10^{-3} $W/cm^2\cdot K$
Coat-side heat-transfer coefficient	10.944×10^{-4} $W/cm^2\cdot K$
Bottom air-supply temperature	333 K
Top air-supply temperature	333 K
Mass-transfer coefficient of solvent 1	1.85×10^{-9} s/cm
Mass-transfer coefficient of solvent 2	1.71×10^{-9} s/cm
Mole fraction of the solvent 1 in the gas	0
Mole fraction of the solvent 2 in the gas	0

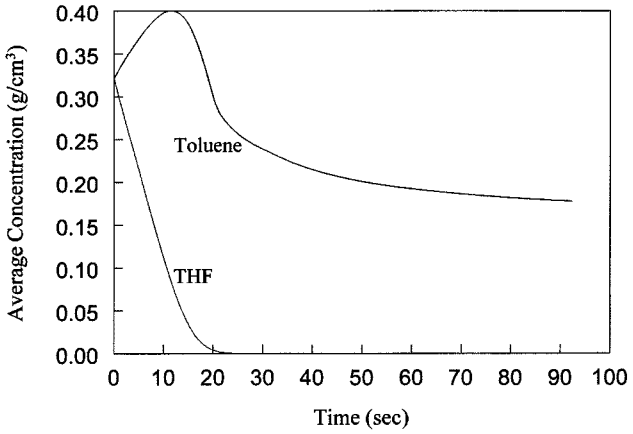

Figure 2. Average concentration of solvents during the drying of PS/toluene/THF system.

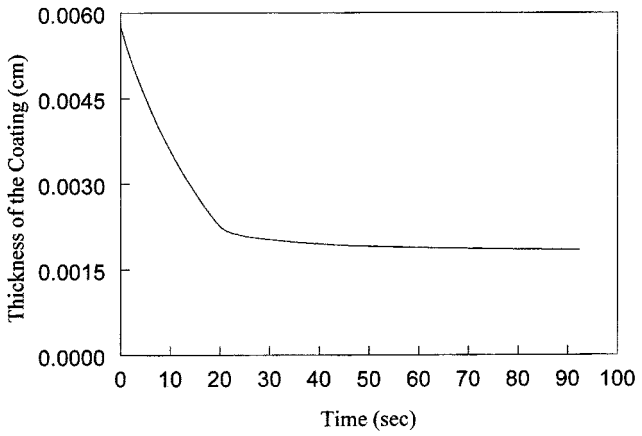

Figure 3. Dimensionless thickness change of the polymer film as a function of time for PS/toluene/THF system.

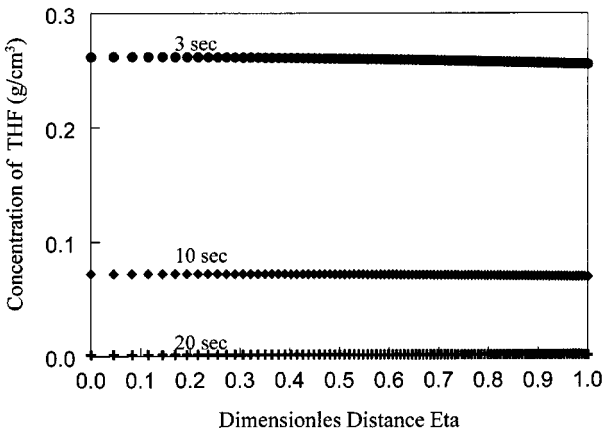

Figure 5. Concentration profiles of THF in the PS/toluene/THF system.

Figure 3 shows the thickness of the coating as a function of time. Coating thickness decreases very rapidly within the first 20 s of drying, and then it levels off to around 0.00185 cm. The temperature of the coating and substrate is shown in Figure 4. A minima in temperature is observed in the first 6 s of drying, since evaporative cooling due to the latent heat of vaporization of the solvent dominates. After 6 s, convective heating of the polymer film and substrate becomes dominant and the temperature of the system approaches oven temperature. Figure 5 shows concentration profiles of THF after 3, 10 and 20 s of drying. No concentration gradient is observed even at the polymer gas interface, which indicates that the drying rate is controlled by external conditions. However very sharp concentration gradients of toluene near the free surface are observed after 20 s of drying, as shown in Figure 6. Note that there are many finite difference grid points in the numerical analysis near the gas interface ($\eta = 1$) that are not apparent in this figure, the number and distribution of the grid points having been optimized to ensure accurate solutions while minimizing the computational time.

These results demonstrate that the overall drying process is controlled by internal resistance after 20 s of drying when all of the THF has disappeared. The existence of sharp gradients at the surface shows the beginning of the skinning phenomena because of the strong diffusional resistance in the polymer film. Note, for the case simulated the concentrations of both toluene and THF in the gas phase are maintained at zero.

In the previous example, the residual amount of toluene trapped in the coating may be unacceptably high. It can be reduced, however, by changing the airflow, temperature, or partial pressure of the more volatile solvent. These parameters constitute the operating conditions for actual manufacturing situations. The following results present the residual amount of toluene after 5,000 s of drying for a range of the operating conditions. Calculations based on changing the air velocity from 0.05 to 1.6 m/s indicate that within that velocity range the heat and mass-transfer coefficients are high enough so that the drying is controlled by diffusion within the polymer film. Consequently, the amount of residual solvent in the film after 5,000 s of drying cannot be significantly reduced by changing the air velocity. On the other hand, increasing the

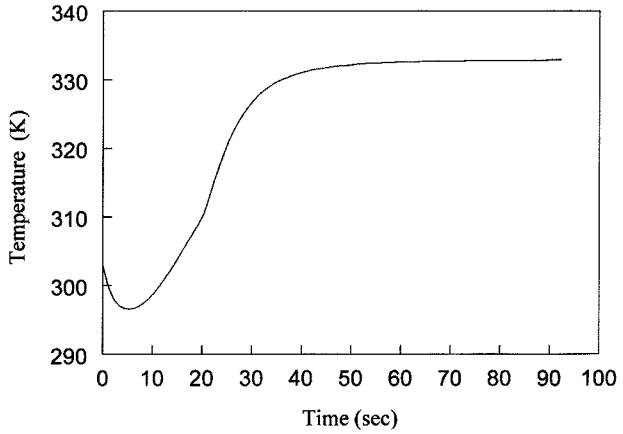

Figure 4. Temperature change of the polymer film and substrate as a function of time for PS/toluene/THF system.

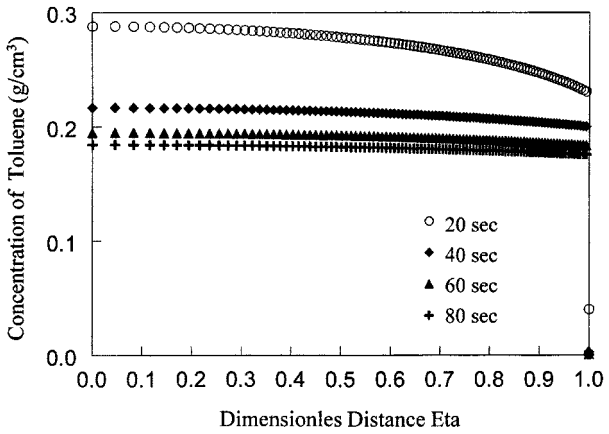

Figure 6. Concentration profiles of toluene in the PS/toluene/THF system.

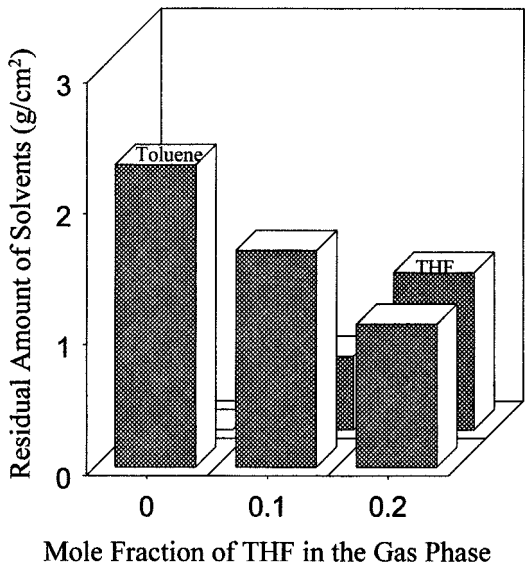

Figure 7. Effect of mole fraction of THF in the gas phase on the residual amount of solvents after 5,000 s of drying for PS/toluene/THF system.

Table 4. Parameters for Polystyrene/Toluene/Ethylbenzene Test System

Initial conditions	
Temperature	370 K
Coating thickness	0.0254 cm
Initial composition of solvent 1	0.39 g/cm^3
Initial composition of solvent 2	0.39 g/cm^3
Substrate parameters	
Heat capacity	1.25 J/g·K
Density	1.37 g/cm^3
Base thickness	0.0508 cm
Coating parameters	
Heat capacity	2.1 J/g·K
Density of polymer	1.083 g/cm^3
Heat of vaporization of the solvent 1	360 J/g
Heat of vaporization of the solvent 2	334.9 J/g
Operating conditions	
Base-side heat-transfer coefficient	0.1136×10^{-2} W/cm^2·K
Coat-side heat-transfer coefficient	0.1136×10^{-2} W/cm^2·K
Bottom air-supply temperature	400 K
Top air-supply temperature	400 K
Mass-transfer coefficient of solvent 1	1.92×10^{-9} s/cm
Mass-transfer coefficient of solvent 2	2.1×10^{-9} s/cm
Mole fraction of the solvent 1 in the gas	0
Mole fraction of the solvent 2 in the gas	0

air temperature from 323 K to 383 K reduces the residual amount of toluene from approximately 3.0 g/cm^2 of film to 0.3 g/cm^2. This dramatic decrease occurs since both the diffusion coefficients and the activities of the solvents increase as the temperatures increase.

One unique feature of the drying of multiple solvent systems is the ability to control the removal of the individual solvents by adjusting the solvent composition of the gas phase. Figure 7 shows the residual amount of both THF and toluene when the mole fraction of the volatile and faster-diffusing component THF in the gas phase is increased from 0 to 0.2. In this case, the residual amount of THF increases while the residual amount of toluene decreases in the coating, since the driving force for the evaporation of THF is reduced by increasing its partial pressure in the oven atmosphere.

The result shown in Figure 7 suggests that the use of a multiple-zone approach in which the concentration of solvents in the gas phase, temperature, and velocity of the gas stream are different in each zone. To illustrate this, we simulated the drying of a polystyrene/toluene/ethylbenzene solution coated on a polyester substrate. The input data used in the simulation are given in Table 4, and the parameters used to predict the self-diffusion coefficients are given in Table 2. Figure 8 shows the average concentration of toluene and ethylbenzene as a function of time when the mole fraction of each solvent in the gas phase is zero. Since the smaller molecule, toluene, has a higher diffusion coefficient and a higher volatility than ethylbenzene, its concentration falls very quickly, while the concentration of ethylbenzene increases to a maximum, when it is trapped in the coating by the skinning effect due to the precipitous fall in diffusion resulting from the lower solvent concentrations at the surface. The residual concentration of ethylbenzene after 1,000 s of drying is 0.02 g/cm^3. If the same solution is dried in an initial oven zone with the nonzero partial pressure of toluene, followed by a second zone with no toluene and with increased air flow and air temperature, then both of the solvents are removed completely, as shown in Figure 9. In the initial zone, the mole fraction of toluene is 0.3, and the heat and mass-transfer coefficients, as well as the air temperature, are the same as those given in Table 4. The second zone starts at 100 s of drying, with no toluene in the oven atmosphere and with heat and mass-transfer coefficients doubled, and the air temperatures on both sides increased by 20 K over the first zone. In this case, most of the ethylbenzene is removed from the coating much faster than toluene. The toluene concentration shows a maxima within 40 s of drying, since the driving force for the evaporation of toluene is reduced by increasing its

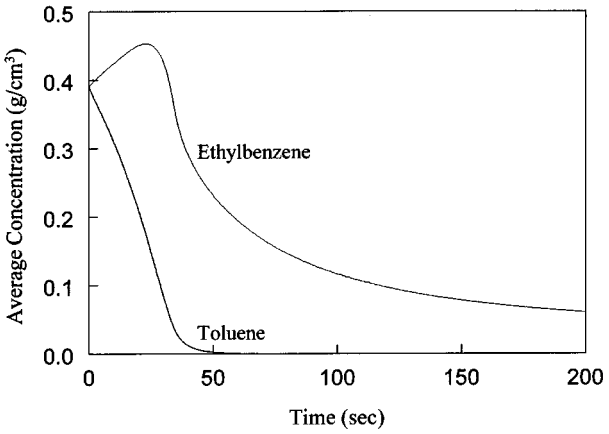

Figure 8. Average concentration of solvents during drying in a single-zone oven for PS/toluene/ethylbenzene system.

Mole fraction of both solvents in the gas phase are zero.

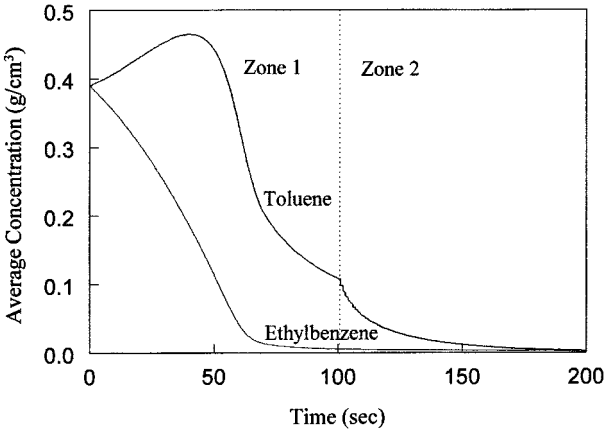

Figure 9. Average concentration of solvents during the drying in a two-zone oven for PS/toluene/ethylbenzene system.

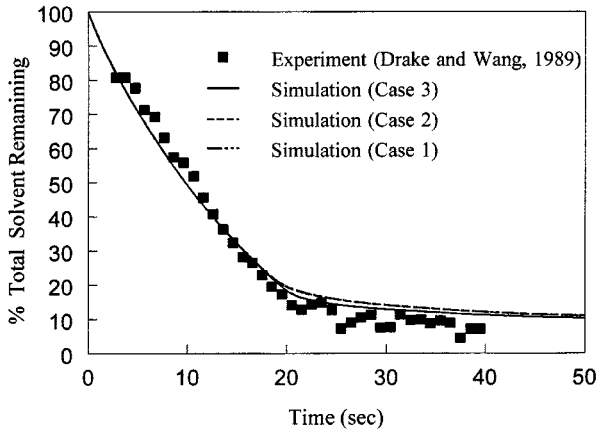

Figure 10. Experimental vs. simulation results for the total residual-solvents level as a function of time for PS/toluene/THF system.

partial pressure in the first oven zone. When the coating enters the second zone, the toluene concentration is 0.11 g/cm^3 and the ethylbenzene concentration is 0.006 g/cm^3. Since the air temperature and air flow are increased and the mole fraction of toluene is zero in the second zone, the rest of the toluene is removed in that zone. The average residual concentration of toluene and ethylbenzene after 1,000 s of drying are 0 and 1.6×10^{-4} g/cm^3, much lower than the residual concentration of ethylbenzene in the coating dried in a single-zone oven, as shown in Figure 8. Consequently, by using several zones and controlling the vapor-phase composition, the removal of all the solvents can be optimized.

A further advantage of multizone drying with multiple solvents is the elimination of coating defects caused by phase separation. If the polymer is totally miscible with component 1 and is not as miscible with less volatile component 2, then component 1 will dry very quickly, leaving the coating rich in component 2, which may phase separate from the polymer and thus cause a defect. By increasing the mole fraction of fast-diffusing component 1, its drying rate can be reduced so that the possibility of a defect causing phase separation can be limited.

Finally, the model is evaluated by comparison with three sets of experimental data. The first experimental data were obtained from the 3M Company (Drake and Wang, 1989) for the PS/toluene/tetrahydrofurane system. The experimental conditions and other input data used in the simulation are given in Table 3. Figure 10 shows that the predictions of the residual amount of solvents in film during the drying are in good agreement with the experimental results. Simulations have been conducted for four alternative approximations of the ternary diffusion coefficients, as indicated in Table 1. In Cases 1 and 2, the assumption employed is that the ratios of the friction coefficients are constant and related to the molar volumes of the species. Therefore diffusivities are a function of the self-diffusion coefficient and the thermodynamic factor (Alsoy, 1998). In Case 1, all four ternary diffusion coefficients are used; however, in Case 2, cross-diffusion coefficients are set to zero. Case 3 represents the commonly used simplest approximation where the cross-diffusion coefficients are equal to zero and the main diffusion coefficients are predicted by the corresponding self-diffusion coefficients without considering the thermodynamic factor. In Case 4, the friction coefficients are set to equal zero in the general formulation of the multicomponent diffusion equations. This results in ternary diffusion coefficients that are functions of both the self-diffusion coefficients and the chemical-potential gradient of each component (Alsoy, 1998). In contrast, for Cases 1 and 2, the main and cross-diffusion coefficients are only functions of the corresponding self-diffusion coefficient and the thermodynamic factor of that component.

As shown in Figure 10, predictions for Cases 1 and 2 are equivalent, while Case 3 predicts a lower residual amount of solvents at later stages of drying. Predictions for all cases are essentially equivalent at the initial stages of drying, since the drying rate is controlled by external conditions. The results in this figure indicate that for the PS/toluene/THF system, the influence of the thermodynamic term is insignificant and the cross-diffusion coefficients are small compared with the main diffusion coefficients, since Cases 1 and 2 produce the same results. The second and third set of experimental data were collected in our laboratory (Alsoy, 1998) under the experimental conditions listed in Table 5. Figure 11 compares the measured total weight of the PS/toluene/benzene system with the predictions from the model. As in the case of PS/toluene/

Table 5. Experimental Conditions for the Drying of PS/Toluene/Benzene and PS/Toluene/Ethylbenzene Systems

System	Initial Thickness (cm)	Initial % wt.	Mass-Transfer Coeff. (s/cm)	Initial Temp. (K)	Oven Temp. (K)
Toluene		45	0.484×10^{-9}		
Benzene	0.115	26	0.477×10^{-9}	293	333
PS		29			
Toluene		27	0.563×10^{-9}		
Ethylbenzene	0.115	66	0.799×10^{-9}	296	353
PS		7			

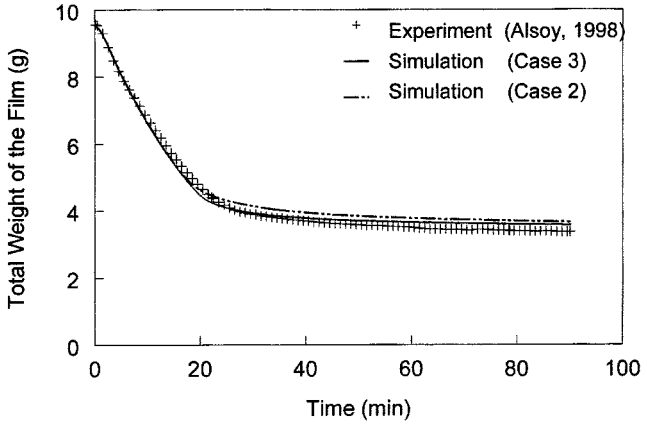

Figure 11. Experimental vs. simulation results for total-weight residual-solvent level as a function of time for PS/toluene/benzene system.

THF, when the main diffusion coefficients are approximated by the self-diffusion coefficients represented by Case 3, the residual amount of solvents is less than the values predicted from Cases 1 and 2. In all cases, however, agreement between the experimental data and the predictions were good.

Finally, predictions for the drying of the polystyrene/toluene/ethylbenzene system are considered. The experimental measurements and the predictions for this system are presented in Figure 12, where the total weight of the film is plotted as a function of time. The results are equivalent for Cases 1, 2 and 3, and it is difficult to distinguish between these three cases on this figure. For all three cases, the predictions are lower than the experimental data between 1,000 and approximately 2,000 s of drying. This disagreement is eliminated when Case 4 is considered. In it, the diffusion coefficients are functions of the self-diffusion coefficients and the chemical-potential gradients of each solvent. Although it is difficult to distinguish the results of Case 4 from the experimental data in Figure 12, the results based on Case 4 are in excellent agreement with the experimental results for the duration of the drying process. In all cases, comparison of the experimental data with the simulation results indicates that the cross-diffusion coefficients are small compared with the main diffusion coefficients.

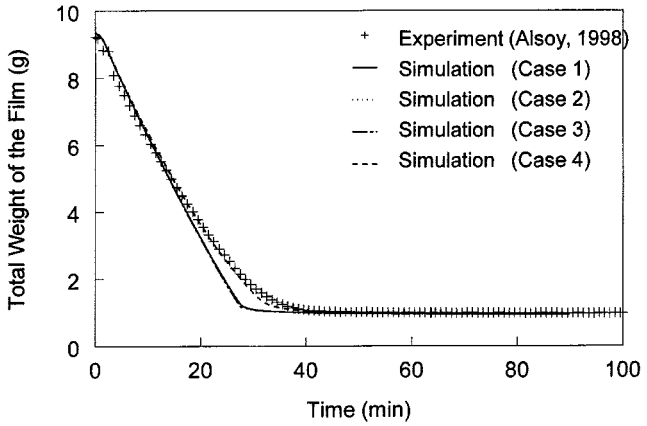

Figure 12. Experimental vs. simulation results for total-weight residual-solvent level as a function of time for PS/toluene/ethylbenzene system.

Conclusions

The multicomponent drying model presented here can be applicable to a large number of important drying processes that involve the drying of multiple solvents. The predictions of the model are in good agreement with the available experimental data. To predict multicomponent diffusion coefficients, two different approximations were derived by assuming that the ratio of the friction coefficients is constant and by setting the friction coefficients to zero. It is not definite which of these approaches is the best, since the results of both are in good agreement with the experiments.

The model establishes a framework for the design and optimization of drying conditions. Optimization involves choosing an objective function such as the final residual solvent level or maximum temperature, and then subjecting the model to a set of constraints such as the operability limits of heaters and fans, zone size, spacing of nozzles, limits in the partial pressure of solvent or temperature at which coating is stable, solubility, skinning factor, or economic factors. For existing drying equipment, drying conditions can be found that meet the objectives and the constraints. For example, the model can predict bubble defects at high temperatures by monitoring the vapor pressure of the solvents at all positions in the film. For the design of new dryers, the model can be used to determine a dryer design that best meets the requirements of the process. The model can also be used to predict the drying process in multizone ovens and as a guide for optimizing the process while minimizing defect formation.

It should be reiterated that the model does have several limitations. The diffusion process is considered to be Fickian in nature, and the molecular transport is not influenced by the buildup of stresses in the polymer film or the relaxation of the polymer chain. Although the ternary Flory–Huggins thermodynamic model was used, any appropriate thermodynamic model could be incorporated into the model. However, nonequilibrium effects, such as the influence of stresses on the thermodynamics and the traversing of glass transition temperatures, have not been included. Many possible defects in the polymer film that are associated with dissolved gases or high stresses are not predicted by the model. However, observation of such defects can be empirically correlated with the outputs from the models, such as the steepness of the concentration gradients at the surface. Obviously, this analysis is only a first step toward an accurate description of multicomponent drying processes. More experimental results are needed to evaluate the model and to clearly determine which model is appropriate for describing such drying processes.

The model has certain unique features that promote the numerical solution of the model equations. Presenting the problem in terms of volume-average velocity reduced the number of equations in the model. Also, using a coordinate transformation and efficient numerical algorithm permitted the computer program to be run successfully on a UNIX-based machine with maximum computational efficiency.

Notation

C_i = dimensionless concentration of component i in the polymer film
$\hat{C}_p$ = specific heat capacity, J/g·K
D_{ii} = main diffusion coefficient, cm^2/s
D_{ij} = cross-diffusion coefficient, cm^2/s
$D^p_{11,o}$ = reference diffusivity calculated at initial composition and temperature in the polymer phase, cm^2/s
$J_i^{\neq}$ = mass diffusive flux of component i with respect to volume-average velocity, $g/cm^2 \cdot s$
k_i = mass-transfer coefficient of component i, s/cm
P_{ii} = partial pressure of component i at the interface, $g/cm \cdot s^2$
P_{ib} = partial pressure of component i in the gas phase, $g/cm \cdot s^2$
R_i = rate of reaction, $g/cm^3 \cdot s$
t = time, s
T_o = initial temperature of the substrate and polymer film, K
T^* = dimensionless temperature
t^* = dimensionless time
$v^{\neq}$ = volume-average velocity, cm/s
$\hat{V}_i$ = partial specific volume of component i, cm^3/g
$X(t)$ = thickness of polymer as a function of time, cm
X^* = dimensionless thickness of polymer

Greek letters

$\Delta \hat{H}_{vi}$ = heat of vaporization of component i, J/g
ρ_i = mass density of component i, g/cm^3
ρ_{io} = initial mass density of component i, g/cm^3
η = dimensionless length variable

Subscripts

p = polymer film
s = substrate

Literature Cited

Alsoy, S., "Modeling of Polymer Drying and Devolatilization Processes," PhD Thesis, The Pennsylvania State Univ., University Park (1998).

Alsoy, S., and J. L. Duda, "Drying of Solvent Coated Polymer Films," *Drying Technol.*, **16**(1&2), 15 (1998).

Bearman, R. J., "On the Molecular Basis of Some Current Theories of Diffusion," *J. Phys. Chem.*, **65**, 1961 (1961).

Blandin, H. P., J. C. David, and J. M. Vergnaud, "Modeling of Drying of Coatings: Effect of the Thickness, Temperature, and Concentration of Solvent," *Prog. Org. Coatings*, **15**, 163 (1987a).

Blandin, H. P., J. C. David, J. M. Vergnaud, J. P. Illien, and M. Malizewicz, "Modeling the Drying Processes of Coatings with Various Layers," *J. Coating Technol.*, **59**, 27 (1987b).

Bristow, G. M., and W. F. Watson, "Cohesive Energy Densities of Polymers: 1. Cohesive Energy Densities of Rubbers by Swelling Measurements," *Trans. Faraday Soc.*, **54**, 1731 (1958).

Cairncross, R. A., R. Jeyadev, R. F. Dunham, K. Evans, L. F. Francis, and L. E. Scriven, "Modeling and Design of an Industrial Dryer with Convective and Radiant Heating," *J. Appl. Polym. Sci.*, **58**, 1279 (1995).

Cairncross, R. A., L. F. Francis, and L. E. Scriven, "Predicting Drying in Coatings that React and Gel: Drying Regime Maps," *AIChE J.*, **42**, 55 (1996).

Daubert, T. E., and R. P. Danner, *Physical and Thermodynamic Properties of Pure Compounds: Data Compilation*, Taylor & Francis, New York (1994).

Drake, M. C., and S. Wang, AIChE Meeting, San Francisco, CA (1989).

Duda, J. L., J. S. Vrentas, S. T. Ju, and H. T. Liu, "Prediction of Diffusion Coefficients for Polymer Solvent Systems," *AIChE J.*, **28**, 285 (1982).

Favre, E., Q. T. Nguyen, R. Clement, and J. Neel, "Application of Flory-Huggins Theory to Ternary Polymer-Solvents Equilibria: A Case Study," *Eur. Poly. J.*, **32**, 303 (1996).

Ferguson, R. D., and E. Von Meerwall, "Free Volume Interpretation of Self Diffusion in Ternary Solutions: *n*-Paraffin-Hexafluorobenzene-cis-4-Polybutadiene," *J. Poly. Sci., B. Poly. Phys.*, **18**, 1285 (1980).

Flory, P. J., *Principles of Polymer Chemistry*, Cornell Univ. Press, Ithaca, NY (1953).

Gutoff, E. B., "Modeling Solvent Drying of Coated Webs Including the Initial Transient," *Drying Technol.*, **14**, 1673 (1996).

Hansen, C. M., "A Mathematical Description of Film Drying by Solvent Evaporation," *J. Oil Colour Chem. Assoc.*, **51**, 27 (1968).

Hong, S., "Molecular Diffusion of Organic Solvents in Multicomponent Polymer Materials," PhD Thesis, The Pennsylvania State Univ., University Park (1994).

Ni, Y. M., "Evaluation of Free Volume Theory for Molecular Diffusion in Polymer Solutions," PhD Thesis, The Pennsylvania State Univ., University Park (1978).

Okazaki, M., K. Shioda, K. Masuda, and R. Toei, "Drying Mechanism of Coated Film Polymer Solution," *J. Chem. Eng. Jpn.*, **7**, 99 (1974).

Shojaeie, S. S., W. B. Krantz, and A. R. Greenberg, "Dense Polymer Film and Membrane Formation via the Dry-Cast Process: Part I. Model Development," *J. Memb. Sci.*, **94**, 255 (1994).

Vrentas, J. S., and J. L. Duda, "Diffusion in Polymer Solvent Systems: I. Re-Examination of the Free Volume Theory," *J. Poly. Sci.*, **15**, 403 (1997a).

Vrentas, J. S., and J. L. Duda, "Diffusion in Polymer Solvent Systems: II. A Predictive Theory for the Dependence of Diffusion Coefficients on Temperature, Concentration and Molecular Weight," *J. Poly. Sci.*, **15**, 417 (1997b).

Vrentas, J. S., J. L. Duda, and H. C. Ling, "Self-Diffusion in Polymer Solvent Systems," *J. Poly. Sci.*, **22**, 459 (1984).

Vrentas, J. S., J. L. Duda, H.-C. Ling, and A.-C. Hou, "Free Volume Theories for Self Diffusion in Polymer Solvent Systems: II. Predictive Capabilities," *J. Poly. Phys.*, **23**, 289 (1985a).

Vrentas, J. S., J. L. Duda, and A. C. Hou, "Enhancement of Impurity Removal from Polymer Films," *J. Appl. Poly. Sci.*, **30**, 4499 (1985b).

Vrentas, J. S., and C. M. Vrentas, "Drying of Solvent Coated Polymer Films," *J. Poly. Sci.: Part B: Poly. Phys.*, **32**, 187 (1994).

Waggoner, R. A., and D. F. Blum, "Solvent Diffusion and Drying of Coatings," *J. Coating Technol.*, **61**, 51 (1989).

Yapel, R. A., "A Physical Model of the Drying of Coated Films," MS Thesis, Univ. of Minnesota, Minneapolis (1988).

Zielinski, J. M., "Free Volume Parameter Estimations for Polymer-Solvent Diffusion Coefficient Predictions," PhD Thesis, The Pennsylvania State Univ., University Park (1992).

Manuscript received Aug. 5, 1998, and revision received Feb. 11, 1999.